Original Research Article

EFFECT OF THE ELECTRONIC STRUCTURE OF PARA-SUBSTITUTED BENZALDEHYDE BENZOHYDRAZONE ON ITS ANTIMICROBIAL ACTIVITY: A DFT ANALYSIS

ABSTRACT

*Bacillus subtilis*is a bacterium that has demonstrated its efficacy across various domains, including industry, agriculture, and commerce, owing to its protective, inhibitory, and biological mechanisms against specific microbes. However, at high concentrations, it can lead to food poisoning and severe infections, resulting in symptoms such as diarrhea and vomiting. Bacterial spores produced by *Bacillus subtilis* can induce conditions like gas gangrene and tetanus.In this context, benzohydrazones are recognized for their antimicrobial activity, particularly against *Bacillus subtilis*. This study aims to elucidate the relationship between the electronic structure of para-substituted benzaldehyde benzohydrazone derivatives and their antimicrobial activity. The goal is to propose a 2D pharmacophore for predicting the antibacterial activity of these derivatives. The quantitative structure-activity relationship (QSAR) approach employed is the KPG method.The electronic structures were optimized using the density functional theory (DFT) method with the B3LYP functional and the 6-31G (d,p) basis set. Charge and local molecular orbitals were considered in the optimization process. The resulting prediction equation (R=98.95%, R^2=97.91%, Adjusted R^2=96.76%, F(5,9)=84.517) derived from multiple linear regression provides the basis for the proposed 2D pharmacophore. This pharmacophore holds potential utility in designing new molecular structures with enhanced activity against *Bacillus subtilis*

Keywords: Bacillus subtilis, QSAR, DFT, KPG method, Hydrazone.

1. INTRODUCTION

Bacillus subtilis, commonly known as hay bacillus or grass bacillus, is a Gram-positive, catalase-positive bacterium. Not only is it the most extensively studied Gram-positive bacterium, but it also serves as a model organism for investigating bacterial chromosome replication and cell differentiation. Widely distributed in soil and the gastrointestinal tracts of ruminants and humans, Bacillus subtilis stands out as a champion bacterium in the production of secreted enzymes employed on an industrial scale by biotechnology companies[1–3]. Certain strains of Bacillus subtilis protect plants from fungal plant pathogens by producing an impressive array of antibiotics, including non-ribosomal lipopeptides (LPs) [4]. This bacterium holds considerable significance in agriculture, trade, and industry, being utilized for diverse purposes such as seed treatment, crop protection, turf foliation, enhancement of peanut seed germination, promotion of nodulation and root growth, and plant nutrition[5, 6].

There is potential for its development as a biological control agent against R. solani in greenhouse cucumber and tomato crops [7]. Several Bacillus species are believed to possess the ability to degrade environmental pollutants, exemplified by Bacillus subtilis' capability to degrade certain pesticides like carbendazim [8, 9] and chlorpyrifos [10]. Additionally, Bacillus subtilis contributes to an increase in the production of gibberellic acids (GAs) and indole acetic acid (IAA), fostering plant growth and enhancing the synthesis of defense molecules such as superoxide dismutase, peroxide, and polyphenol oxidase [11]. Furthermore, Bacillus exhibits inhibitory effects on pathogens through the production of antibiotic lipopeptides[12, 13]. Despite its numerous benefits, Bacillus subtilis has adverse effects and poses a moderate potential danger to humans. It has been implicated in the etiology of food toxico-infections, with high concentrations leading to diarrhea and/or vomiting [14]. The production of extracellular enzymes and toxins by Bacillus subtilis contributes to its pathogenicity in humans. Moreover, resistance to several antimicrobial drugs presents a challenge for its treatment [15].

In the laboratory, the chemistry of nitrogenous compounds has long been a subject of extensive study [16]. Hydrazones, a class of nitrogenous compounds, are particularly valuable in drug design due to the presence of an azomethine proton -NHN=CH- in their structure [17]. The physical, chemical, and biological properties that allow the understanding and prediction of the activity or behavior of molecules in the environment are embedded in the structure of these compounds. Molecular modeling, especially QSAR/QSPR (Quantitative Structure-Activity/Property Relationships), is a widely used technique for predicting the properties/activities of chemical systems from their molecular structures [18][19]. Over the decades, QSAR has played a pivotal role in drug development, encouraging scientists in the pharmaceutical field to explore relationships between molecular parameters and properties beyond activity [20]. To comprehend a mechanism of action, researchers can examine the relationships between the descriptors of the QSAR model and toxicity or other activities [21]. The assumption that the molecular structure of a series of compounds contains essential information about the factors responsible for their physical, chemical, or biological properties has led chemoinformaticians to extensively employ QSAR/QSPR to study the biological activity of various compounds [19, 22–27]. Presently, one of the greatest challenges in QSAR/QSPR studies is assessing the reliability of the mechanistic interpretation of the identified relationships [28].

Given the adverse effects of Bacillus subtilis on humans, its resistance to antimicrobials, the pharmacological properties of hydrazones, and the significance of QSAR, there is an urgent need to identify hydrazone molecules that can more effectively control Bacillus subtilis. Therefore, the overarching objective of our project is to conduct QSAR on a series of hydrazone molecules

and propose pharmacophores that can act more effectively on Bacillus subtilis, with the aim of combating diarrhea, vomiting, and food poisoning caused by this pathogen.

2. MODEL, METHODS AND CALCULATIONS

2.1 Model

$$\log(C_{MIC}) = a + bM_{D_i} + c\log\left[\sigma_{D_i}/(ABC)^{1/2}\right] + \sum_j \left[e_j Q_j + f_j S_j^E + s_j S_j^N\right] + \sum_j \sum_m \left[h_j(m)F_j(m) + x_j(m)S_j^E(m)\right] + + \sum_j \sum_{m'} \left[r_j(m')F_j(m') + t_j(m')S_j^N(m')\right] + \sum_j \left[g_j\mu_j + k_j\eta_j + o_j\omega_j + z_j\varsigma_j + w_j Q_j^{\max}\right] \quad \text{(Eq.1)}$$

with a, b, c, e_j, f_j, s_j, $h_j(m)$, $x_j(m)$, $r_j(m')$, $t_j(m')$, g_j, k_j, o_j, z_j and w_j are constants, M_{D_i} is the mass of the drug, σ_{D_i} is its symmetry number, ABC is the product of the moments of inertia of the drug around the three main axes of rotation, Q_j is the net charge of the atom j, S_j^E and S_j^N are, respectively, the total electrophilic and nucleophilic atomic superdelocalizations of atom j, $F_j(m)$ and $F_j(m')$ are respectively the electron populations (Fukui index) of the occupied (m) and vacant (m′) molecular orbitals (OMs) located on the atom j, $S_j^E(m)$ is the atomic electrophilic superdelocalizability of the OM (m) localized on the atom j, μ_j is the local electronic chemical potential of the atom j, η_j is the local atomic hardness of the atom j, ω_j is the local atomic electrophilicity of atom j, ς_j is the local atomic softness of the atom j, $Q_j^{\max}$ j is the maximum amount of electronic charge that atom j can accept from another site, and Ok is the orientation parameter of the kth substituent [29, 30].

2.2 Methods

To find the relationship between the electronic structure and the inhibitory concentration of the series of para-substituted benzaldehyde benzohydrazone derivatives, we used a methodology widely explained in the articles [31–41]. The results obtained were presented following a routine methodology. So this article contains only the results and discussion because the method and calculations have been discussed in several articles [31–41].

2.3 Selection of the molecules

The para-substituted benzaldehyde benzohydrazone derivatives used are from reference [42]. The general formula and the antibacterial activities (mean inhibitory concentration: CMIC) of these molecules are represented respectively in figure 1 and table 1.

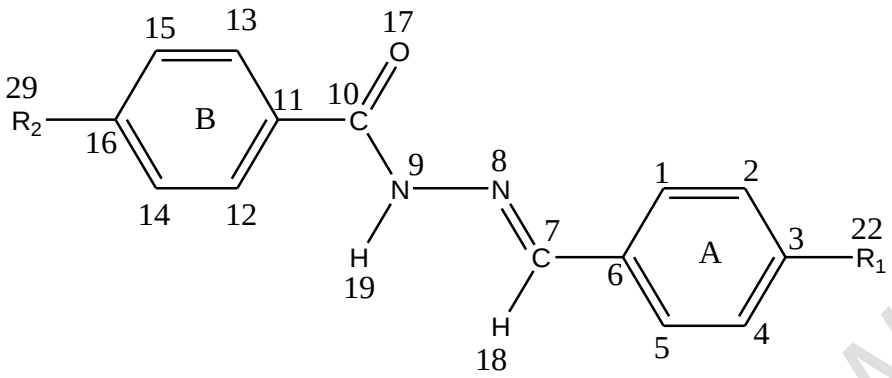

Fig 1. General structure of para-substituted benzaldehyde benzohydrazone derivatives

Table 1. Molecules of para-substituted benzaldehyde benzohydrazone derivatives with the decimal logarithm of their average inhibitory concentrations [log(C_{MIC})].

N°	R_1	R_2	log(C_{MIC})
A_1	-H	-H	-5.35
A_2	-H	$-CH_3$	-5.37
A_3	-H	$-OCH_3$	-5.40
A_4	-H	-Cl	-5.41
A_5	-H	-OH	-5.38
A_6	$-OCH_3$	-H	-5.40
A_7	$-OCH_3$	$-CH_3$	-5.42
A_8	$-OCH_3$	$-OCH_3$	-5.45
A_9	$-OCH_3$	-Cl	-5.45
A_{10}	$-OCH_3$	-OH	-5.41
A_{11}	$-NO_2$	-H	-5.42
A_{12}	$-NO_2$	$-CH_3$	-5.45
A_{13}	$-NO_2$	$-OCH_3$	-5.47
A_{14}	$-NO_2$	-Cl	-5.48
A_{15}	$-NO_2$	-OH	-5.45

We observed that the amplitude is low. This could be a limitation of this study. To provide a comprehensive example of how to implement the KPG method, a study with a higher amplitude should be conducted.

2.4 Calculations

The Gaussian program was employed for the geometrical optimizations [43]of the fifteen structures of para-substituted benzaldehyde benzohydrazone derivatives using the density functional theory (DFT) and the 6-31G(d,p)/B3LYP basis. Regarding the D-CENT QSAR program [44, 45]it was utilized to calculate the local atomic reactivity indices for the various atoms in the shared skeleton of the distinct para-substituted benzaldehyde benzohydrazone molecules. To exclude atoms with weak coefficients, the Statistica 10 program was applied, enabling the execution of multiple linear regression [46]. The common skeleton

of the fifteen antibacterial molecules under investigation is illustrated in Figure 2, including the numbering of its different atoms.

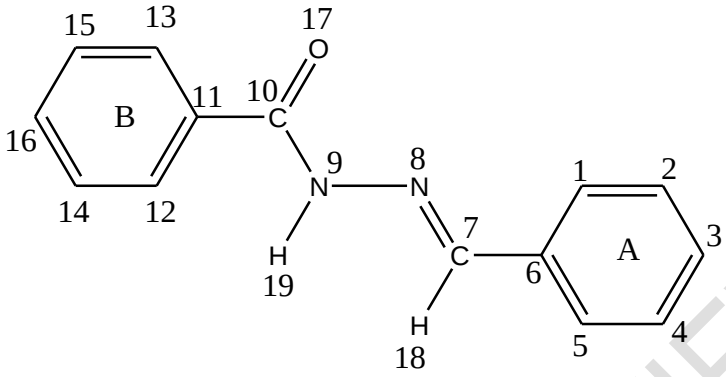

Fig. 2. Common skeleton of para-substituted benzaldehyde benzohydrazone derivatives.

3. RESULTS AND DISCUSSION

3.1 Results

After multiple linear regression (MLR), we obtained the following model:

$$log(C_{MIC}) = 2.17 + 6.13Q_5 - 12.0Q_{10} + 0.38\omega_{13} + 0.69F_{19}(HOMO)* + 0.27Q_{14} \text{(Eq. 2)}$$

$$log(C_{MIC}) = 2.17 + 6.13Q_5 - 12.0Q_{10} + 0.38Q_{13}^{max} + 0.69F_{19}(HOMO)* + 0.27Q_{14} \text{Bon}$$

With R = 98.95%; R² = 97.91%; Adjusted R² = 96.76%; F(5.9) = 84.517; (*p* =*.0000003*) and SD = 0.007. No outliers were detected and no residuals outside the 2 limit.

According to this prediction model, the activity of para-substituted benzaldehyde benzohydrazone derivatives on *Bacillus subtilis* potentially depends on five (05) local atomic reactivity indices: Q_5 is the net charge of the C_5 carbon atom of the aromatic ring A, Q_{10} is the net charge of the carbon atom C_{10} of the carbonyl group, Q_{13}^{max} is the maximum amount of electronic charge that atom C_{13} of the aromatic ring Bmayreceived, $F_{19}(HOMO)*$ is the Fukui index of the first highest occupied molecular orbital (HOMO)* located on the hydrogen atom H_{19}, Q_{14} is the net charge of the carbon atom C_{14} of the aromatic ring B.

Tables 2 and 3group respectively the beta coefficients and the correlation matrix between the five explanatory variables of the model.

Table 2. Statistical parameters of the different indices of the regression model

Variables	p-value	Beta coefficients
Q_5	0.0000001	1.041
Q_{10}	0.000002	-0.695
Q_{13}^{max}	.002	0.277
F_{19}(HOMO)*	.02	0.139
Q_{14}	.05	0.139

Table 3. Correlation matrix of the different variables of the model

	Q_5	Q_{10}	Q_{13}^{max}	F_{19}(HOMO)*	Q_{14}
Q_5	1.00				
Q_{10}	0,058	1.00			
Q_{13}^{max}	0,056	0,210	1.00		
F_{19}(HOMO)*	0,012	0,069	0,005	1.00	
Q_{14}	0,0001	0,228	0,256	0,002	1.00

Figure 3shows that there is a good correlation of observed versus calculated values and that almost all points are inside the 95% confidence interval.

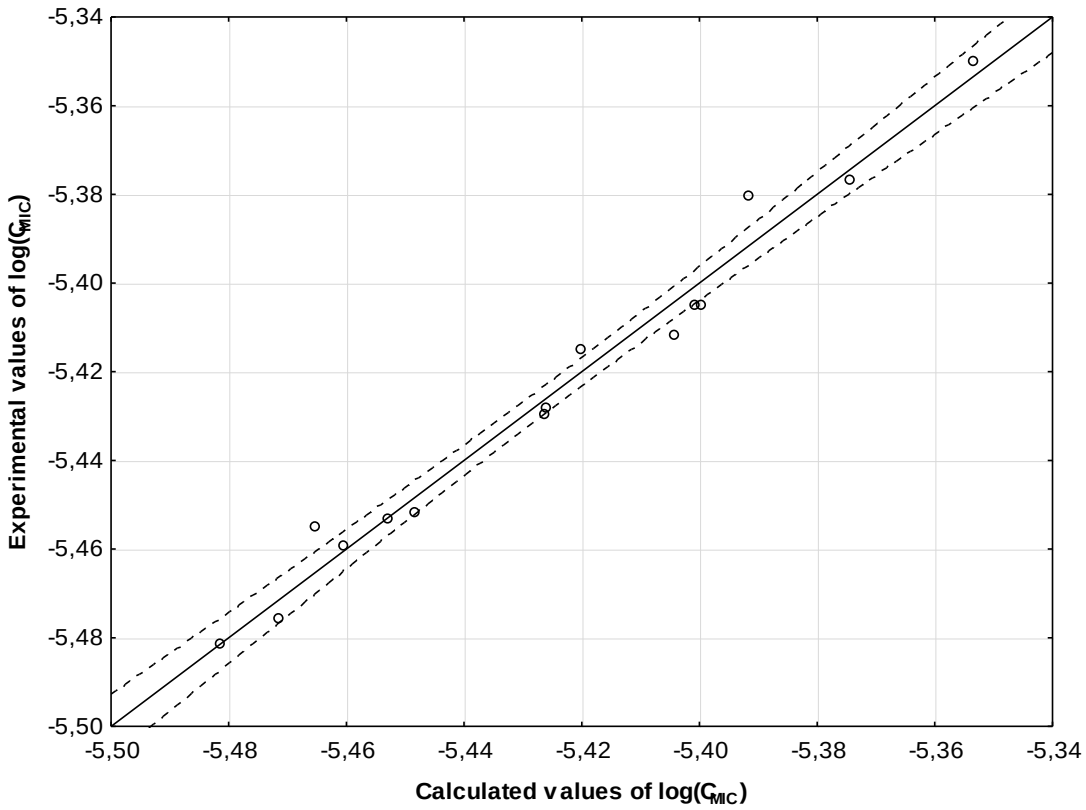

Fig. 3. Prediction plot of the experimental values of log(C_{MIC}) against the values estimated from Eq. 1. The dashed lines indicate the 95% confidence interval.

Table 4 shows the local MO structure of atoms with reactivity indices appearing in Eq. 1 (see Fig. 2). Nomenclature: Molecule (HOMO) / (HOMO-2)* (HOMO-1)* (HOMO)* - (LUMO)* (LUMO+1)* (LUMO+2)*.

Table 4. The local molecular orbitals of atoms 5,10, 13, 19 and 14 of the developed model

Molecules	Atom (C_5)	Atom (C_{10})	Atom (C_{13})	Atom (H_{19})	Atom (C_{14})
A_1 (59)	54π55π5π9-60π61π62π	57σ58π59-60π61σ64π	52π57π58-60π61π62π	45σ53σ54σ-62σ63σ65σ	56π57π58π-60π61π62π
A_2 (63)	58π59π63π-64π65π66π	61π62π63π-64σ65π68π	60π61π62-64π65π67π	48σ57σ58-66σ67σ69σ	60π61π62π-64π65π67π
A_3 (67)	63π66π67-68π69π70π	62π65π66-68π69π72π	65π66π67-68π69π70π	51σ61σ62-69σ70σ71σ	65π66π67π-69π70π71π
A_4 (67)	62π64π67π-68π69π70π	65σ66π67π-68σ69π72π	63π65π66-68π69π70π	51σ61σ62-70σ74σ75σ	63π65π66π-68π69π70π
A_5 (63)	59π62π63π-64π65π66π	61π62σ63-64π65σ68π	61π62π63-64π65π66π	49σ57σ58-65σ66σ69σ	61π62π63π-66π67π68π
A_6 (67)	62π65π67π-68π69π70π	64σ66π 67σ-68π69σ72σ	63π64π66-68π69π70π	39σ52σ61-69σ70σ71σ	60π64π66π-68π69π70π
A_7 (71)	65π66π71π-72π74π76π	69σ70σ71π-72π73σ74π	68π69π70-72π73π74π	41σ55σ65-73σ74σ75σ	68π69π70π-72π75π76π
A_8 (75)	70π72π75π-76π77π78π	73σ74σ75π-76σ77π78π	73π74π75-76π78π79π	43σ58σ69-77σ79σ81σ	73π74π75π-78π79π80π
A_9 (75)	71π73π75π-76π77π78π	73σ74π75π-76 77σ81π	71π72π74-76π77π78π	57σ58σ69-77σ78σ80σ	72π73π74π-76π78π79π
A_{10} (71)	66π68π71π-72π73π74π	69σ70σ71π-72π 73π74σ	69π70π71-72π74π75π	40σ56σ65-73σ77σ78σ	68π69π70π-73π75π76π
A_{11} (70)	65π66π70π-71π72π73π	68σ69π70π-71σ72π74π	67π68π69-72π74π75π	54σ65σ66-73σ75σ78σ	67π68π69π-72π75π76π
A_{12} (74)	69π70π74π-75π76π77π	72σ73π74π-75σ76σ77π	72π73π74-76π78π79π	57σ69σ70-77σ79σ81σ	71π72π73π-76π79π80π
A_{13} (78)	74π77π78π-79π80π81π	71σ76π77π-79π80σ81σ	76π77π78-80π81π82π	60σ73σ74-81σ83σ85σ	76π77π78π-83π84π85π
A_{14} (78)	73π74π78π-79π80π81π	76π77σ78σ-79σ80π82π	76π77π78-80π83π85π	71σ73σ74-81σ82σ83σ	75π76π77π-80π83π84π
A_{15} (74)	70π73π74π-75π76π77π	67σ72π 73π-75π76σ77π	72π73π74-76π77π78π	58σ69σ70-77σ78σ79σ	72π73π74π-78π79π80π

3.2 Discussion

Global statistical parameters of the developed model

- Obtaining an adjusted R^2 coefficient = 96.76% proves that the antimicrobial activity of para-substituted benzaldehyde benzohydrazone molecules on *Bacillus subtilis* is strongly correlated with the five local atomic reactivity indices.

- Obtaining a Fischer probability F(5.9) = 84.517 > tabulated F(5.9) = 3.48, shows that the developed model is statistically significant and that there is a 95% chance that there is a real relationship between the antimicrobial activity of the para-substituted benzaldehyde-benzohydrazone molecules and the local atomic reactivity indices.
- The p-value obtained (*p=.0000003< .05*) also confirms that the developed multiple linear regression model is statistically significant.

Correlation between the different indices of the multiple linear regression model

Table 3 shows us the correlations between the five local atomic reactivity indices of the developed model. The analysis of the values in this table shows that there is a low correlation (practically less than 50%) between the different indices. This proves the interdependence between these indices in predicting the antimicrobial activity of para-substituted benzaldehyde benzohydrazone molecules.

Statistical parameters of the five indices of the established model

The values of the beta coefficients in Table 2 show that the most important index in the antimicrobial activity of Bacillus Subtilis is the net charge Q_5 of atom 5 and the order of priority of the different indices in the model is as follows: $Q_5 > Q_{10} > Q_{13}^{max} > F_{19}(HOMO) * > Q_{14}$

All p-values for the five local atomic reactivity indices in Table 2 are less than 5%. Therefore, all these indices are statistically significant and can be used for variable-by-variable analysis.

Variable-by-variable analysis of the prediction model indices:

The lower C_{MIC}, the better the antimicrobial activity. Therefore, better antimicrobial activity of para-substituted benzaldehyde benzohydrazone derivatives would be associated with low value of negative net charges Q_5 and Q_{14} with positive coefficients, low positive value of Q_{13}^{max} with a positive coefficient, to a low value of the Fukui index F_{19} (HOMO)* positive with a positive coefficient and a high value of the net load Q_{10} positive with a negative coefficient.

Atoms 5, 10, and 14 are carbon atoms. However, the net charges of atoms C_5 and C_{14} are negative, while the net charge of atom C_{10} is positive. This discrepancy can be attributed to the fact that atoms 5 and 14 are carbons belonging to aromatic rings, thus rich in electrons. In contrast, atom 5 is a carbon doubly bound to an oxygen atom, depleting it in electrons. The net charge Q_{14} of the atom is influenced by the nature of the substituent R_2 attached to the C_{16} carbon of the aromatic ring B (figure 2). Analyses suggest that both atom 5 and atom 14 could contribute to antimicrobial activity through cation-anion or cation-π interactions, including the π-π interactions involving the C_{14}-

C_{16} and C_5-C_6 atoms. On the other hand, the C_{10} carbon atom would establish anion-cation or anion-π interactions.

Atom 13 is a carbon atom. low value of Q_{13}^{max} suggest that this atom is not prone to receive extra charge. Therefore atom 13 is probably facing an electron-deficient center. Atom 13 must interact with an electron acceptor. This interaction may be of the π-alkyl or alkyl-alkyl type.

Atom 19 is a hydrogen atom bound to the nitrogen atom N_9. The local molecular orbitals (MOs) of this atom are all sigma (σ) in nature. For better inhibitory activity of the compounds a low positive value of F_{19}(HOMO)* is necessary. For this, the orbital of the H_{19} atom must interact with an electron-deficient center through its highest occupied sigma local molecular orbital.

Based on these analyses, we propose a 2D pharmacophore in figure 4, indicating the sites where substituents should be attached to enhance the antimicrobial activity of the compounds in general and their inhibitory activity on Bacillus subtilis in particular.

Fig.4. Pharmacophore 2D pour l'inhibition de *Bacillus subtilis*

4. CONCLUSION

The utilization of the Klopman-Peradejordi-Gómez (KPG) method has allowed us to establish a prediction model for the antimicrobial activity of para-substituted benzaldehyde benzohydrazone derivatives. This predictive model demonstrates a 98.95% likelihood of a correlation between the antimicrobial activity of these para-substituted benzaldehyde benzohydrazone molecules and the five potential local atomic reactivity indices. The pharmacophore, derived from a variable-by-variable analysis of this model, highlights specific atoms in the common backbone of para-substituted benzaldehyde benzohydrazone derivatives where bioisosteres could be strategically grafted to enhance their antimicrobial activity. Leveraging this 2D pharmacophore, we can propose potential structures for antimicrobially active derivatives of para-substituted benzaldehyde benzohydrazone.

REFERENCES

1 Paul, S. I., Rahman, Md. M., Salam, M. A., Khan, Md. A. R. and Islam, Md. T. (2021) Identification of marine sponge-associated bacteria of the Saint Martin's island of the Bay of Bengal emphasizing on the prevention of motile Aeromonas septicemia in Labeo rohita. *Aquaculture***545**, 737156 https://doi.org/10.1016/j.aquaculture.2021.737156

2 Rahman, M. M., Paul, S. I., Akter, T., Tay, A. C. Y., Foysal, M. J. and Islam, M. T. (2020) Whole-Genome Sequence of Bacillus subtilis WS1A, a Promising Fish Probiotic Strain Isolated from Marine Sponge of the Bay of Bengal. *Microbiol Resour Announc* (Dunning Hotopp, J. C., ed.) **9** https://doi.org/10.1128/MRA.00641-20

3 Errington, J. and Aart, L. T. van der. (2020) Microbe Profile: Bacillus subtilis: model organism for cellular development, and industrial workhorse. *Microbiology***166**, 425–427 https://doi.org/10.1099/mic.0.000922

4 Cawoy, H., Debois, D., Franzil, L., De Pauw, E., Thonart, P. and Ongena, M. (2015) Lipopeptides as main ingredients for inhibition of fungal phytopathogens by Bacillus subtilis/amyloliquefaciens: Lipopeptides as inhibitors of phytopathogens. *Microbial Biotechnology***8**, 281–295 https://doi.org/10.1111/1751-7915.12238

5 GIRAUD Romain. (2019) Bacillus : une bactérie auxiliaire pour la santé du gazon Par Romain GIRAUD -6 mai 20190

6 Turner, J. T. (1991) Factors Relating to Peanut Yield Increases After Seed Treatment with *Bacillus subtilis*. *Plant Dis.***75**, 347 https://doi.org/10.1094/PD-75-0347

7 Demeule Elizabeth. (2020) Effet répressif de Bacillus subtilis et de Bacillus pumilus envers Rhizoctonia solani sur tomate et concombre de serre. *Mémoire de maitrise, Québec, Canada*
8 Zhang, H., Zhang, Y., Hou, Z., Wu, X., Gao, H., Sun, F., et al. (2014) Biodegradation of triazine herbicide metribuzin by the strain *Bacillus* sp. N1. *Journal of Environmental Science and Health, Part B***49**, 79–86 https://doi.org/10.1080/03601234.2014.844610
9 Salunkhe, V. P., Sawant, I. S., Banerjee, K., Wadkar, P. N., Sawant, S. D. and Hingmire, S. A. (2014) Kinetics of degradation of carbendazim by B. subtilis strains: possibility of in situ detoxification. *Environ Monit Assess***186**, 8599–8610 https://doi.org/10.1007/s10661-014-4027-8
10 El-Helow, E. R., Badawy, M. E. I., Mabrouk, M. E. M., Mohamed, E. A. H. and El-Beshlawy, Y. M. (2013) Biodegradation of Chlorpyrifos by a Newly Isolated *Bacillus subtilis* Strain, Y242. *Bioremediation Journal***17**, 113–123 https://doi.org/10.1080/10889868.2013.786019
11 Chowdappa, P., Mohan Kumar, S. P., Jyothi Lakshmi, M. and Upreti, K. K. (2013) Growth stimulation and induction of systemic resistance in tomato against early and late blight by Bacillus subtilis OTPB1 or Trichoderma harzianum OTPB3. *Biological Control***65**, 109–117 https://doi.org/10.1016/j.biocontrol.2012.11.009
12 Shafi, J., Tian, H. and Ji, M. (2017) *Bacillus* species as versatile weapons for plant pathogens: a review. *Biotechnology & Biotechnological Equipment***31**, 446–459 https://doi.org/10.1080/13102818.2017.1286950
13 Ongena, M. and Jacques, P. (2008) Bacillus lipopeptides: versatile weapons for plant disease biocontrol. *Trends in Microbiology***16**, 115–125 https://doi.org/10.1016/j.tim.2007.12.009
14 Patrick Berche. Une histoire des microbes. *Livre*
15 (2018) Rapport d'évaluation finale de Bacillus cereus et de Bacillus subtilis. *Rapport, Canada*
16 Benmansour Née Baba Hamed Yamina. Synthèse, étude physico-chimique et ac tivité biologique des complexes de cuivre et/ou nickel dérivés d'Hydrazone et Thiadiazole. *Thèse*
17 Suman Bala, Goldie Uppal, Anu Kajal, Sunil Kamboj and Vaibhav Sharma. (2013) Hydrazones as Promising Lead with Diversity in Bioactivity-therapeuticPotential in Present Scenario. *International Journal of Pharmaceutical Sciences Review and Research***18**, 65–74
18 Katritzky, A. R. (2000) Advances in Quantitative Structure Property Relationships. Volume 2 Edited by Marvin Charton (Pratt Institute) and Barbara I. Charton (St. John's University). JAI Press Inc.: Stamford, CT. 1999. xi + 257 pp. $109.50. ISBN 0-7623-0067-1. *J. Am. Chem. Soc.***122**, 1846–1846 https://doi.org/10.1021/ja995762c
19 Kpotin, G. A., Bédé, A. L., Houngue-Kpota, A., Anatovi, W., Kuevi, U. A., Atohoun, G. S., et al. (2019) Relationship between electronic structures and antiplasmodial activities of xanthone derivatives: a 2D-QSAR

approach. *Struct Chem***30**, 2301–2310 https://doi.org/10.1007/s11224-019-01333-w
20 Grover, M., Singh, B., Bakshi, M. and Singh, S. (2000) Quantitative structure–property relationships in pharmaceutical research – Part 1. *Pharmaceutical Science & Technology Today***3**, 28–35 https://doi.org/10.1016/S1461-5347(99)00214-X
21 Sizochenko, N., Gajewicz, A., Leszczynski, J. and Puzyn, T. (2016) Causation or only correlation? Application of causal inference graphs for evaluating causality in nano-QSAR models. *Nanoscale***8**, 7203–7208 https://doi.org/10.1039/C5NR08279J
22 Kankinou S Gautier, Gaston Kpotin, Jean-Baptiste Mensah and Juan-Sebastián Gómez-Jeria. (2019) Quantum-Chemical Study of the Relationships between Electronic Structure and the Affinity of Benzisothiazolylpiperazine Derivatives for the Dopamine Hd2l and Hd3 Receptors. *The Pharmaceutical and Chemical Journal***6**, 73–90
23 Puzyn, T., Leszczynski, J. and Cronin, M. T. (Eds.). (2010) Recent Advances in QSAR Studies: Methods and Applications, Springer Netherlands, Dordrecht https://doi.org/10.1007/978-1-4020-9783-6
24 Furrow E. Michael and Myers G. Andrew. (2004) Practical Procedures for the Preparation of N-tert-Butyldimethylsilylhydrazones and Their Use in Modified Wolff-Kishner Reductions and in the Synthesis of Vinyl Halides and gem-Dihalides **126**
25 Bardieu Atchade, Salomé D.S. Kpoviessi, Raymond H. Fatondji, Léon A. Ahoussi, Joachim Gbenou, Georges C. Accrombessi, et al. (2015) Synthesis, Purity Verification and Comparison of Antiplasmodial and Antitrypanosomal Activities of Hydrazone Derivatives and Corresponding Thiosemicarbazones. *Journal of Pharmaceutical, Chemical and Biological***3**, 279–294
26 Juan S. Gómez-Jeria, Andrés Robles-Navarro, Gaston Assongba Kpotin, Nicolás Garrido-Sáez and Nelson Gatica-Díaz. (2020) Some remarks about the relationships between the common skeleton concept within the Klopman-Peradejordi-Gómez QSAR method and the weak molecule-site interactions. *Chemistry Research Journal***5**, 32–52
27 Houngue, M. T. A. K., N'bouke, M., Atchade, B., Doco, R. C., Kuevi, U. A., Kpotin, G. A., et al. (2018) Quantum Chemical Studies of Some Hydrazone Derivatives. *CC***06**, 1–14 https://doi.org/10.4236/cc.2018.61001
28 Organisation for Economic Co-operation and Development. (2007) Guidance document on the validation of (quantitative) structure-activity relationship [(Q)SAR] models **69**
29 Gomez-Jeria, J. S. and Valdebenito-Gamboa, J. (2015) A quantum-chemical analysis of the antiproliferative activity of N-3-benzimidazolephenylbisamide derivatives against MGC803, HT29, MKN45 and SW620 cancer cell lines. *Der Pharma Chemica***7**, 103–121

30 Robles-Navarro, A. and Gómez Jeria, J. (2016) A quantum-chemical analysis of the relationships between electronic structure and cytotoxicity, GyrB inhibition, DNA supercoiling inhibition and antitubercular activity of a series of quinoline–aminopiperidine hybrid analogues. *Der Pharma Chemica***8**, 417–440
31 Gómez Jeria JS. (1982) La Pharmacologie Quantique. *Boll. Chim. Farmac.***121**, 619–25. French
32 Gómez-Jeria JS. (2013) Flores-Catalán M. Quantum-chemical modeling of the relationships between molecular structure and In vitro multi-step, multimechanistic drug effects. HIV-1 Replication Inhibition and Inhibition of Cell Proliferation as Examples. *Canadian Chemical Transactions***1**, 215–37
33 Gómez-Jeria JS. (2013) Elements of molecular electronic pharmacology. *Ediciones Sokar, Santiago de Chile*
34 Bruna-Larenas T and Gómez-Jeria JS. (2012) A DFT and semiempirical model-based study of opioid receptor affinity and selectivity in a group of molecules with a morphine structural core. *Int. J. Med. Chem.* 1-16,Article ID 682495
35 Leal MS, Robles-Navarro A, and Gómez-Jeria JS. (2015) A density functional study of the inhibition of microsomal prostaglandin E2 Synthase-1 by 2-aryl substituted quinazolin-4(3H)-one, pyrido[4,3-d]pyrimidin-4(3H)-one and pyrido[2,3- d]pyrimidin-4(3H)-one derivatives. *Der Pharm. Lett.***7**, 54–66
36 Barahona-Urbina C, Nuñez-Gonzalez S and Gómez-Jeria JS. (2012) Model-based quantum chemical study of the uptake of some polychlorinated pollutant compounds by Zucchini subspecies. *J. Chil. Chem. Soc.***57**, 1497–503
37 Gómez-Jeria JS. (1989) Modeling the drugreceptor interaction in quantum pharmacology in molecules. In Physics, Chemistry, and Biology. *J. Maruani Editor, Netherlands: Springer*
38 Gómez-Jeria JS. (2013) New set of local reactivity indices within the Hartree-Fock-Roothaan and density functional theory frameworks. *Canad. Chem. Trans***1**, 25–55
39 Gómez-Jeria JS. (1983) On some problems in quantum pharmacology I. The partition functions. *Int. J. Quant. Chem.***23**, 1969–72
40 Gómez-Jeria JS,. (2015) A DFT analysis of the inhibition of carbonic anhydrase isoforms I, II, IX and XII by a series of benzenesulfonamides and tetrafluorobenzenesulfonamides **2**, 66
41 Gómez-Jeria JS. (2016) Tables of proposed values for the orientational parameter of the substituent I. Monoatomic, Diatomic, Triatomic, n-CnH2n+1, O-n-CnH2n+1, NRR', and Cycloalkanes (With a Single Ring) Substituents. *Res. J. Pharmac. Biol. Chem. Sci.***7**, 288–94

42 Jankulovska M.S. and Dimova V. (2019) Pratical application of QSAR technique for prediction of biological activity of selected hydrazones. *Journal of Agricultural, Food and Environmental Sciences, JAFES***73**
43 Frisch MJ, Trucks GW, Schlegel HB, Scuseria GE, Robb MA, Cheeseman JR, et al. (2007). *Rega N. G03 Rev. E.01. Gaussian, Pittsburgh, PA, USA*
44 Gómez-Jeria JS. (2009) An empirical way to correct some drawbacks of mulliken population analysis. *J. Chil. Chem. Soc.***54**, 482–85
45 Gómez-Jeria JS. (2014) D-Cent-QSAR: A program to generate local atomic reactivity indices from Gaussian 03 log files. *v. 1.0. Santiago, Chile*
46 (1984) Statistica v. 8.0. 2300 East 14 th St. Tulsa, OK 74104. *USA*